Nature of prominences and their role in Space Weather
Proceedings IAU Symposium No. 300, 2013
B. Schmieder, J.-M. Malherbe & S. T. Wu, eds.

doi:10.1017/S1743921313010764

On the nature of the prominence - corona transition region

Susanna Parenti[1] **and Jean-Claude Vial**[2]

[1]Royal Observatory of Belgium - STCE,
3 Av. Circulaire, Brussels, Belgium
email: s.parenti@oma.be

[2]Institut d'Astrophysique Spatiale, Université Paris Sud - CNRS,
Orsay Cedex, France
email: jean-claude.vial@ias.u-psud.fr

Abstract. Due to the complexity of their environment, prominences properties are still a matter of controversy. Prominences cool and dense plasma is suspended in the hot corona by a magnetic structure poorly known. Their thermal insulation from the corona results in a thin geometrical interface called prominence-corona-transition-region (PCTR). Here we will review the main properties of such a region as derived primarily from observations. We will introduce the thermal structure properties, describe the fine structure together with the Doppler-shift and width properties of lines of the emitting plasma. We will introduce the proposed interpretations of such observations and the limits of our knowledge imposed by the present instrumentation. We will conclude with a perspective for the future observations of the PCTR.

Keywords. prominences, UV-EUV, transition region, spectroscopy

1. Introduction

Solar prominences have the peculiar property of being made of cool plasma (mainly at chromospheric temperatures) embedded in a magnetic structure suspended in the corona. As in the case of the chromosphere, this implies the existence of an interface region with the corona, where the temperature of the plasma rises from about 7000 K to 1×10^6 K. Such a region is called prominence-corona transition region (PCTR).

Prominences are found above some of the photospheric neutral lines. At large scales, it is known that the magnetic field is at about 30 deg angle with the underlying neutral line, which itself is parallel to the main body of the prominence. This means that the overall lateral PCTR is at about 30 deg with the magnetic field.

Prominences are formed by a collection of thin magnetic flux tubes (about 200 km wide) filled by cool plasma. Looking at, for example, Hα images (Figure 1), we see that a single flux tube is only partially filled by the prominence plasma. The rest may be filled by coronal material. This means that there exists also a PCTR inside the flux tube which has the temperature gradient almost aligned with the magnetic field. Considering that the efficiency of the thermal conduction depends on the angle between the magnetic field and the temperature gradient directions, it is clear that the large and small scale PCTRs may have different properties (see for example Heinzel and Anzer 2001). At present the only information we have on the field-aligned temperature gradient comes from modeling, as the observations are limited in spatial resolution. The PCTR is, in fact, observed by the EUV instruments which, until now, could not resolve single threads. With the launch of the new NASA/IRIS mission, such discrepancy is reduced and new results on this topic are expected.

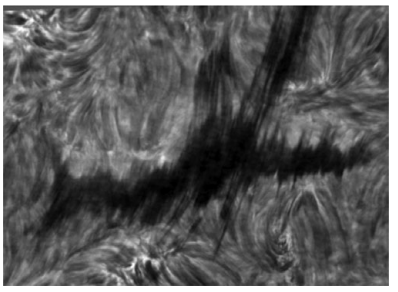

Figure 1. A segment of a filament observed in Hα by the Swedish 1-m Solar Telescope (SST). The fine structure is only partially filled by cool plasma. Courtesy O. Engvold.

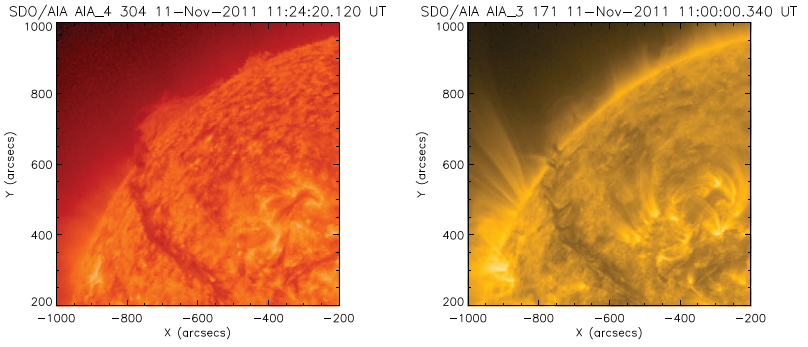

Figure 2. A prominence (left) and its transition region (right) observed by SDO/AIA in, respectively, the EUV He II 304 Å and Fe IX 171 Å wavebands.

The first property we discuss is the general appearance of the PCTR. Figure 2 shows the same prominence observed co-temporally in the wavebands He II 304 Å (sampling the low transition region, left plot) and Fe IX Å (sampling the high transition region-corona, right plot). Off-limb the two images are clearly different: in the He II image the prominence is brighter than the background, indicating that the PCTR is emitting between 2 and 8×10^4 K; in the Fe IX image the prominence is faintly visible in emission, suggesting that if present, the prominence emission at about 0.8 MK is quite low or absent, as the background corona emission is already low. In Sect. 2 we will further discuss the temperature structure of the PCTR and mention a few recent theoretical works on this topic. On the disk, the two images show a dark prominence. This aspect is mainly due, for the 304 Å channel, to He II self absorption, but also by the absorption of the spectral lines by the hydrogen and helium continua produced by the neutral H and He, and singly ionized He plasma of the prominence (see e.g. Chiuderi Drago *et al.* 2001, Chiuderi Drago and Landi 2002) and, at least for the 171 Å case, by the absence or weak emission of the PCTR with respect to the background quiet Sun. In Sect. 3 we will further discuss the PCTR properties as derived from on-disk filament observation. From these first properties of the PCTR emission we already understand that the mass of this region should be reduced with respect to that of the prominence core. However, the PCTR has its role to maintain the stability of the whole prominence. As we will see (Sect. 3), it is a dynamic region and its local and global emissions contribute to the radiative losses of the structure. We will conclude this paper with Sect. 4, with a few important recommendations for the future studies of the PCTR.

https://doi.org/10.1017/S1743921313010764 Published online by Cambridge University Press

2. The thermal structure

The PCTR at the interface with the background corona is probably a thin layer with a steep gradient of temperature, as the thermal conduction perpendicular to the magnetic field is not efficient to thermalize the plasma. As mentioned, deriving the PCTR properties from the observations is important for understanding the physics of the whole prominence. As it has been shown by several works, the emerging emission of H (see e.g. Heinzel *et al.* 2001) and He (see e.g. Labrosse *et al.* 2002) from a prominence is affected by the presence or not of a transition region.

The prominence is an extremely complex environment which, in certain cases, imposes the use of some simplifications in the modeled physics. The close interaction between observation and modeling works is a key to improve this issue. Observers have the role of providing modelers with the best suitable information to properly constrain and simplify their work. We give some examples of such interaction in this section.

To infer the thermal structure of the PCTR we need to have observations in a wide temperature range, typically from about 10^4 to 10^6 K. The inversion of the data is done using the differential emission measure (DEM) technique applied to the optically thin UV-EUV emission of the PCTR. The DEM is a measure of the amount of plasma at each temperature ($DEM(T) = n_e^2 dh/dT$, where T is the electron temperature, n_e the electron density and h the line of sight). Details of this technique are given in Labrosse *et al.* (2010).

Due to the properties of this technique, only off-limb prominence DEMs have been derived so far. For a better constrain of the inversion, a large number of spectral lines has to be used and only few results are present in the literature (e.g. Wiik, Dere, and Schmieder 1993, Cirigliano, Vial, and Rovira 2004, Parenti *et al.* 2010, Parenti and Vial 2007, Parenti, Vial, and Lemaire 2008, Gunár *et al.* 2011).

Figure 3 left shows one of the latest inferred prominences DEM (Parenti and Vial 2007). It was obtained inverting more than forty spectral lines intensity from elements in different stages of ionization measured by SOHO/SUMER on October 18 1999. On the same day a similar observation was obtained on the quiet Sun, with the purpose of comparing the DEM profiles of the two regions. The DEM of the quiet Sun is shown on Figure 3 right. As the DEM profile in temperature is shaped, at a given time, by the physical process acting inside a structure, this comparison is necessary to understand if and how much the PCTR behaves differently from the corona-chromosphere transition region (CCTR). As we see from the figure this is the case: the PCTR has smaller DEM values almost everywhere (beside the coronal part, which will be discussed later) and a different DEM gradient at similar temperatures (including a different value of temperature where the DEM minimum is located). The interpretation of these differences is still under study and some results are presented hereafter.

In addition to the comparison of the thermal structure of the PCTR to the CCTR, further investigations need to work out if and how the thermal structure (DEM) of different quiescent prominences differ from each other. This would allow to identify those properties typical to all prominences, which then can be used in constraining their modeling. From the few results published on this topic, the answer is not ready. This is because of the limitations, for example, in the data: the temperature coverage, the lack of corona background subtraction. Figure 3 left shows no data below $logT = 4.4$ (at this temperature the emission starts to become optically thick in most lines). Other data may have different limitations (see for example Gunár *et al.* 2011) which would produce a DEM having a different gradient at such temperature. At present we also often lack the suitable data needed for the estimation of the coronal contribution surrounding the

https://doi.org/10.1017/S1743921313010764 Published online by Cambridge University Press

prominence. This was the case for the structure of Parenti and Vial (2007): the peak of the DEM at 1MK in Figure 3 left is almost certainly the background corona, while the gradient of the high transition region part of the DEM is contaminated by the background corona. These limitations need to be overcome in order to advance in prominences investigations.

Thermal structure and energy balance. One of the motivations to reduce the uncertainties on the DEM constraints is its use to estimate the total radiative losses of the PCTR (e.g. Parenti and Vial 2007). The stable emission of a prominence in quiescent conditions suggests an almost continuous input of energy into the structure. At present there are several candidate processes for such sources (thermal conduction, waves, chromospheric irradiation, see Heinzel and Anzer 2012 for the cool core), but none of them seems to be sufficient to compensate the radiative losses from the prominence core to the low PCTR (up to about 10^5 K, at higher temperature the thermal conduction is by now the best candidate for this compensation). Particularly critical is the energy budget in the core, where most of the emission is concentrated. To make the problem more complicated, the core emission should be treated using non-local thermodynamic equilibrium (NLTE) treatment of the radiative transfer. The estimate of the core's radiative losses is still not complete today, and the bridge with the radiative losses of the PCTR is missing. For this reason an extension of the DEM at lower temperature ($logT < 4.5$, where possible) and a better estimate of the core losses would allow to have the full temperature information on the energy balance.

A possible solution to this problem is the use of the H-Ly lines (e.g. Heinzel *et al.* 2001, Stellmacher and Wiehr 2008, Gunár *et al.* 2011, Vial *et al.* 2012, Schwartz *et al.* 2012) as they are formed at different heights from the core to the PCTR. Unfortunately most of the available data miss the profile of the H-Lyα line, which can put better constraints to the results. Including this line in the future observations is strongly recommended.

In addition, the newly launched NASA/IRIS spectrometer is observing the intense Mg II line, which until now was not included in the core losses budget known (however, Mg II modeling can be found, for example, in Vial 1982, Paletou, Vial, and Auer 1993). As far as radiative losses are concerned, according to Heinzel *et al.* 2013, the inclusion of Mg II losses decreases dramatically the radiative-equilibrium temperature at very low pressures. This situation is much different at high pressures (opacities) where the Mg II contribution is negligible, as it is the case in the CCTR.

We also point out that the high transition region and coronal part of the thermal emission of prominences is scarcely known due to the difficulty of isolating it from the

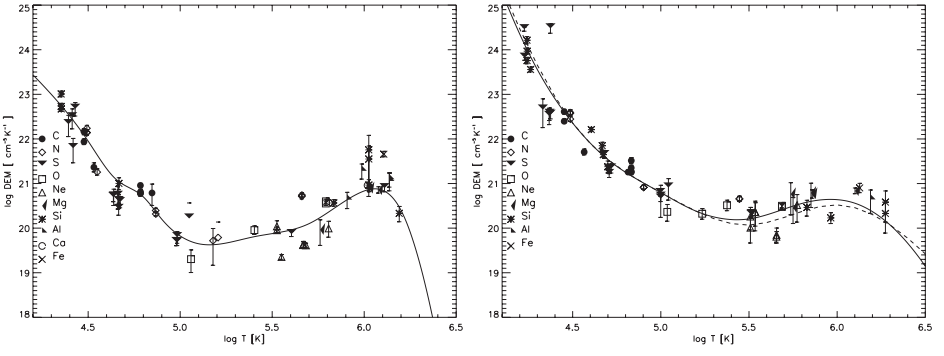

Figure 3. Logarithm of the DEM as function of the logarithm of temperature for the PCTR (left) and the quiet Sun (right, the double curve originate from different data). From Parenti and Vial (2007).

https://doi.org/10.1017/S1743921313010764 Published online by Cambridge University Press

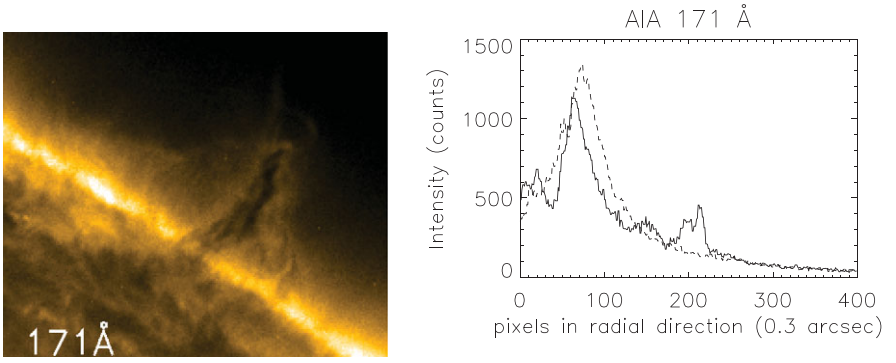

Figure 4. Left: prominence observed by SDO/AIA 171 Å on the 22 June 2010. A weak but clear emission is seen inside the structure surrounding the central part seen in absorption. Right: radial cut across the prominence (solid line) and off-limb corona at the side of the structure (dotted line). An emission above the background is clearly visible around pixel 200. From Parenti *et al.* (2012).

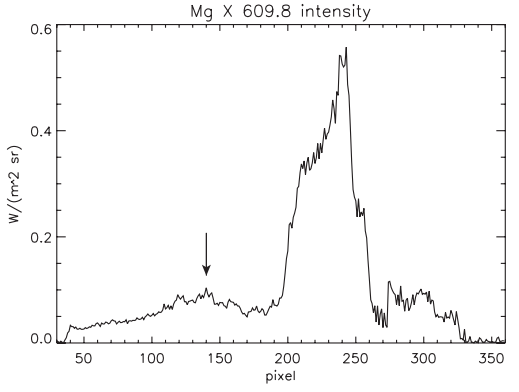

Figure 5. Mg X 609 Å line intensity across a prominence observed on November 11, 2011 with SOHO/SUMER. The limb is located at around pixel 240. The off-limb signal is affected by absorption by neutral hydrogen inside the denser part of the prominence (around pixels 150-200). A weak emission is seen between the pixels 120-150 as indicated by the vertical arrow. Parenti *et al.* 2013.

background/foreground off-limb emission. On this topic, the new images produced by the NASA/SDO high sensitivity AIA EUV instrument have revealed that the PCTR emits also at quite high temperature and, consequently it could be more massive than previously thought (Figure 4). Parenti *et al.* (2012) have investigated this aspect using a combination of AIA data analysis and simulation. They concluded that the emission seen in the AIA 171 Å channel is due to Fe IX, and not from cooler lines which also fall into the instrument waveband. They estimated a PCTR emission up to 4×10^5 K. Kucera *et al.* (2012) found signatures of emission in a prominence even at hotter temperatures (Fe X, Fe XI), suggesting that more work on this topic should be done.

These new results stimulate further studies which will better quantify the thermal distribution of the high temperature part of the PCTR. Preliminary results on spectroscopic data from SOHO/SUMER (Parenti *et al.*, 2013) of the off-limb prominence shown in Figure 2, seems to indicate a weak PCTR emission above the background level at temperature close to 1MK, as shown in Figure 5. Further investigations are under way.

https://doi.org/10.1017/S1743921313010764 Published online by Cambridge University Press

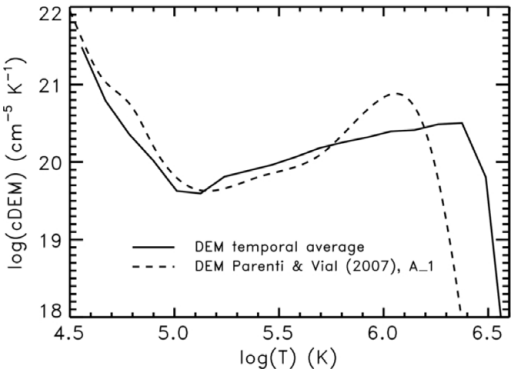

Figure 6. Solid line: Logarithm of the DEM as function of the logarithm of temperature for the PCTR, averaged over the time simulation and space. The dashed line is the DEM derived from observations by Parenti and Vial (2007). From Luna, Karpen, and DeVore (2012).

Thermal structure and prominence formation. The observed thermal structure of the PCTR has been used to study and constrain models of the formation of prominences. For instance, Luna, Karpen, and DeVore (2012) have recently simulated the formation of the fine scale of a prominence by the thermal non-equilibrium process inside a 3D shared arcade (see also DeVore, Antiochos, and Aulanier 2005). Their outputs included the DEM which was compared to that derived from observations by Parenti and Vial (2007). The result is well constrained in all the transition region, as it is shown in Figure 6. Some differences between the two DEMs are located at coronal temperature. But as mentioned earlier, this is probably because the Parenti and Vial (2007) DEM includes the background emission while, as pointed out by Luna, Karpen, and DeVore (2012), the high temperature part of the theoretical DEM they show was not completely representative of the whole coronal arcade they had in the model.

3. Fine structure and dynamics

PCTR from on-disk filament observations. In view of its (supposedly) extremely small thickness, the PCTR is difficult to detect tangentially when the prominence is seen at the limb (it would require a sub-arcsec resolution, still not achieved in the UV from space, except from VAULT, see below). This direct observation is equally difficult when the prominence is seen on the disk as a filament. But one can use the fact that one sees the fibril/thread structuring from above, which allows for precise cuts accross the aligned structures. For instance, the unique filament image obtained by VAULT (Vial *et al.* 2012, Figure 7) in the Lα line (formed at the bottom of the PCTR) displays a fine fibril (or thread) structure at the level of the spatial resolution (0.3 arcsec). This does not mean that there is no fibril or thread with a smaller cross-section. But this also could indicate that we have a relatively large PCTR common for smaller numerous (cool) threads within the 0.3 arcsec span. Until the advent of the results from IRIS and its slit-jaw images (e.g. Si IV), there is no way to firmly conclude. With the VAULT Lα data, Vial *et al.* (2012) found a typical thread cross-section of one arcsec with a minimum of 0.4 arcsec, slightly larger than the 0.3 arcsec cross-sections of the Hα fibrils (Lin *et al.* 2005, Lin *et al.* 2008). For this limiting case, one could conclude that the individual thread PCTR is 0.05 arcsec (or about 40 km). But for the bulk of the observed threads, the large cross-section can also imply that we have a PCTR common to a set of threads.

https://doi.org/10.1017/S1743921313010764 Published online by Cambridge University Press

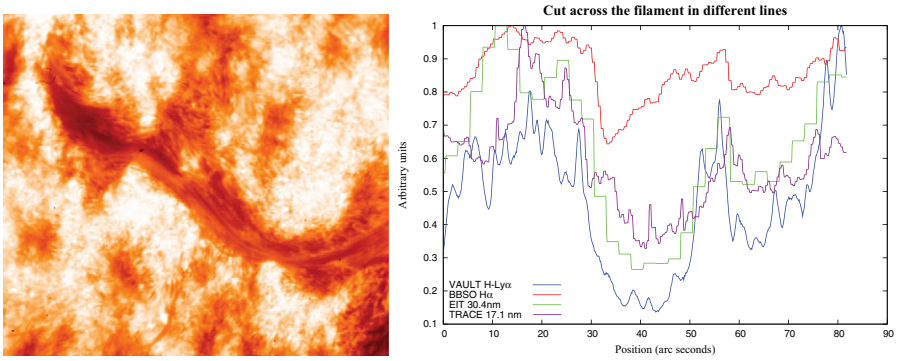

Figure 7. Left: a detail of the filament observed by VAULT. Right: A cut of the filament in different spectral lines: VAULT H-Lα is the bottom curve, BBSO Hα is the upper curve, EIT 304 Å and TRACE 171 Å are the middle curves. The arbitrary units are obtained by dividing the cut intensity by its maximum value. From Vial *et al.* (2012).

High spatial IRIS observations (launched in 2013) of prominences and filaments should bring more light on this issue.

A major feature of the VAULT observations (Vial *et al.* 2012) was the confirmation of filament extensions, as shown in Figure 7 (see e.g. Heinzel, Schmieder, and Tziotziou 2001). Such extensions are of the order of 10 arcsec (and less) and can be noticed in the UV and EUV absorbed lines. At this stage, it is tempting to consider them as the bottom of the global PCTR (up to 3×10^4 K). It should also be remembered that the VAULT observations concern an active region filament whose properties may differ from a quiescent one.

Filling factor. There are different ways for overcoming the difficulties of "direct" observations of the PCTR. One is to derive a (volume) filling factor through the measurement of the EM (and consequently the average of the square of the density) and the derivation of the local density from appropriate line ratios. Values of the order of 0.02 have been obtained by Mariska, Doschek, and Feldman (1979) and even lower ones by Cirigliano, Vial, and Rovira (2004) with the implication of a very high number of threads along the line-of-sight (up to 35). Similar results were obtained from the interpretation of the intensity, shift and width distributions : Wiik, Dere, and Schmieder (1993) also found 30 threads in the PCTR and later on (Wiik *et al.* 1999) 20 threads at the N V temperature. However, one should be aware of the many assumptions relevant to these different methods. EM and density derivations are often limited by photon noise and the intensity vs. velocity distributions can lead to different results.

Modeling the small scale PCTR. Beside the observational limitation of the PCTR, important progress has been made in the past years by the effort of combining observation and modeling works. For example, Gunár *et al.* (2011) have developed a 2D multi-thread model of prominences which includes small line-of-sight velocity and solves a multi-level NLTE problem for the hydrogen spectral lines. They tested different prominence conditions by comparing simulated and observed Lyman line profiles and DEMs. Using these two complementary quantities, it was possible to link the properties at the base of the transition region with those at higher temperatures. Their results showed good agreement between data and simulation, even though multiple solutions were still compatible with the data. An example of the DEMs comparison is shown in Figure 8. Even if this work gives a set of solutions, it goes in the right direction to better constrain prominence fine scale modeling with a PCTR (see also Gunár paper in this volume).

https://doi.org/10.1017/S1743921313010764 Published online by Cambridge University Press

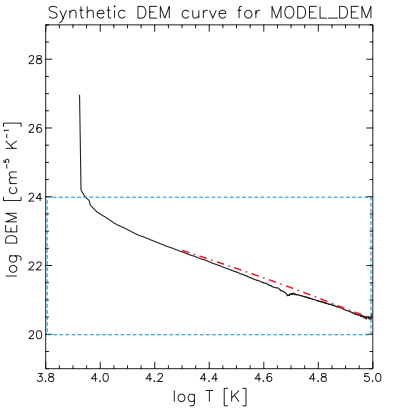

Figure 8. Synthetic DEM curve (solid black line) for one realization of the multi-thread prominence with 10 threads. The red dash-dotted line represents the DEM derived from the observations of the June 8, 2004 prominence. From Gunár *et al.* (2011)

Similarly to what is observed in the prominence core the PCTR is dynamic showing, for example, bulk motion and turbulence. We have to remember that we cannot reach the same spatial information as the dynamics observed for the core. This opens the questions if the two are related and if they are governed by the same mechanisms. This will have implications also in the question of the fine scale structure: is each thread surrounded by its own PCTR or a common PCTR exists for a bunch of threads (e.g. Pojoga 1994, Vial *et al.* 2012).

Bulk motions. The bulk motions of the PCTR have been studied both by following the paths of absorption features (due to H, He I and He II continua, e.g. Schmieder *et al.* 2008) and Doppler-shifts (e.g. Labrosse *et al.* 2010). The feature tracking technique found motions with similarities to the counter-streaming flow observed with the Hα instruments. However, in general both techniques give variable results ($5 < v < 40$ km/s) which are affected by limitations of the data inversion methods and instruments. Again, we expect the new IRIS spectrometer to have better performances.

Non-thermal velocities. At the spatial resolution of unresolved threads, the spectral profiles of the optically thin UV-EUV lines have a width greater than their thermal Doppler width. This property is also present in the CCTR but, as the latest results show, their path in temperature are not exactly the same (and they can change from prominence to prominence, see e.g. Stellmacher, Wiehr, and Dammasch 2003). We show this in Figure 9 where are plotted the non-thermal velocities of the prominence on the left, and the quiet Sun on the right. This extra width of the spectral line could be interpreted as turbulence, waves or/and the superposition of line-of-sight flows of unresolved structures. We still have no answer for that, but the high spatial resolution of IRIS will certainly contribute to this topic. The different runs of the velocities with temperature shown in Figure 9, once properly interpreted, will let us understand better in what and why the CCTR and PCTR are different.

The small scale dynamics observed in the core have been recognized to have their role in the formation and stability of the prominence. What about the observed dynamics of the PCTR? One step forward could be done once we understand if there is a link between what are observed in the core and in the PCTR. Similarly to the case of the DEM, for the non-thermal velocities the complete path in temperature is missing. Only few km/s are derived in the coolest part of the structure, while about 10 km/s are derived at the base of the transition region. Recent results by Park *et al.* (2013) obtained Ca II and Hα

https://doi.org/10.1017/S1743921313010764 Published online by Cambridge University Press

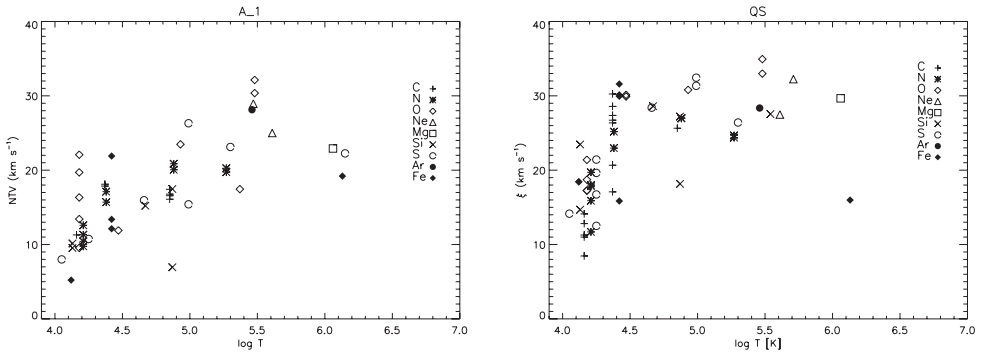

Figure 9. Non-thermal velocities as function of the logarithm of the temperature for the PCTR of the same prominence and quiet Sun of Figure 3. From Parenti and Vial (2007).

non-thermal velocities between 4 and 11 km/s, in agreement with the picture already proposed (for further recent results see also Ramelli *et al.* 2012) of non-thermal velocities increasing when moving outside the core.

4. Conclusion

In this paper we have briefly gone through some of open questions concerning the properties of the PCTR. We are aware that this layer is more complex than what we previously thought and to progress we need a common effort from the observation and modeling sides. The lack of high resolution observations contributes to limit our investigations concerning the thermal structure across and along the fine prominence threads, together with a continuous link with the thermal properties of the prominence core. This is also true for the dynamics studies, which use data affected by spatial and temporal integration. We are looking forward for the IRIS first results, but also for the future Solar Orbiter ESA mission, which will resolve about 100 km on the Sun and fraction of seconds in exposure time. To better understand which are the dominant physical processes governing the PCTR, to understand if they are common to the core, it would require to have co-temporal spectroscopic observations which cover a wide temperature range. This is still not completely achieved.

Even if we haven't gone in detail through the progress in the modeling of the PCTR, we have seen that the new multi-threads models appear to be promising. But more effort should be put by modelers, by extending the complexity of the physics they use, starting with including a PCTR reaching higher temperatures than the typical 10^5 K. In addition, observations reveal that threads are not static and a variety of prominence internal motions exists. These are scarcely taken into account in modeling, beside the aspect of waves propagation, which is giving interesting results (see other works in this book).

Here we have not discussed the magnetic field properties in the PCTR. We could summarize saying that at present there are no observations able to detect such a weak field. However there are proposals for using, e.g. the Hanle effect in the H-Lα line which, eventually, will sample the $2-3\times10^4$ K part of the PCTR. The access to such measurements will already be a step forward in the PCTR knowledge.

https://doi.org/10.1017/S1743921313010764 Published online by Cambridge University Press

References

Chiuderi Drago, F., Alissandrakis, C. E., Bastian, T., Bocchialini, K., & Harrison, R. A. 2001, *Solar Phys.* 199, 115.

Chiuderi Drago, F. & Landi, E. 2002, *Solar Phys.* 206, 315.

Cirigliano, D., Vial, J.-C., & Rovira, M. 2004, *Solar Phys.* 223, 95.

DeVore, C. R., Antiochos, S. K., & Aulanier, G. 2005, *ApJ* 629, 1122.

Gunár, S., Parenti, S., Anzer, U., Heinzel, P., & Vial, J.-C. 2011, *A&A* 535, A122.

Gunár, *et al.* 2013, this volume.

Heinzel, P., Schmieder, B., Vial, J.-C., & Kotrč, P. 2001, *A&A* 370, 281.

Heinzel, P., Schmieder, B., & Tziotziou, K. 2001, *ApJ* 561, L223.

Heinzel, P. & Anzer, U. 2001, *A&A* 375, 1082.

Heinzel, P., Schmieder, B., Fárník, F., Schwartz, P., Labrosse, N., Kotrč, P., Anzer, U., Molodij, G., Berlicki, A., DeLuca, E. E., Golub, L., Watanabe, T., & Berger, T. 2008, *ApJ* 686, 1383.

Heinzel, P. & Anzer, U. 2012, *A&A* 539, A49.

Kucera, T. A., Gibson, S. E., Schmit, D. J., Landi, E., & Tripathi, D. 2012, *ApJ* 757, 73.

Labrosse, N., Heinzel, P., Vial, J.-C., Kucera, T., Parenti, S., Gunár, S., Schmieder, B., & Kilper, G. 2010, *Space Sci. Revs* 151, 243.

Labrosse, N., Gouttebroze, P., Heinzel, P., & Vial, J.-C. 2002, *Solar Variability: From Core to Outer Frontiers*, 506, 451.

Lin, Y., Engvold, O., Rouppe van der Voort, L., Wiik, J. E., & Berger, T. E. 2005, *Solar Phys.* 226, 239.

Lin, Y., Martin, S. F., Engvold, O., Rouppe van der Voort, L. H. M., & van Noort, M. 2008, *Adv. Sp. Res.* 42, 803.

Luna, M., Karpen, J. T., & DeVore, C.R. 2012,*ApJ* 746, 30.

Mariska, J. T., Doschek, G. A., & Feldman, U. 1979, *ApJ* 232, 929.

Paletou, F., Vial, J.-C., & Auer, L. H. 1993, *A&A*, 274, 571.

Parenti, S., Vial, J.-C., & Lemaire, P. 2008, *Adv. Sp. Res.*, 41, 144.

Parenti, S. & Vial, J.-C. 2007, *A&A*, 469, 1109.

Parenti, S., Schmieder, B., Heinzel, P., & Golub, L. 2012, *ApJ*, 754, 66.

Parenti, S., Vial, J.-C., Schmieder, B., & Heinzel, P. 2013, in preparation.

Park, H., Chae, J., Song, D., Maurya, R. A., Yang, H., Park, Y.-D., Jang, B.-H., Nah, J., Cho, K.-S., Kim, Y.-H., Ahn, K., Cao, W., & Goode, P. R. 2013, *Solar Phys.* 72.

Pojoga, S. 1994, *IAU Colloq. 144: Solar Coronal Structures*, 357.

Ramelli, R., Stellmacher, G., Wiehr, E., & Bianda, M. 2012, *Solar Phys.* 281, 697.

Schmieder, B., Bommier, V., Kitai, R., Matsumoto, T., Ishii, T. T., Hagino, M., Li, H., & Golub, L. 2008, *Solar Phys.*, 247, 321.

Schwartz, P., Schmieder, B., Heinzel, P., & Kotrč, P. 2012, *Solar Phys.* 281, 707.

Stellmacher, G., Wiehr, E., & Dammasch, I. E. 2003, *Solar Phys.* 217, 133.

Stellmacher, G. & Wiehr, E. 2008, *A&A* 489, 773.

Vial, J. C. 1982, *ApJ* 254, 780.

Vial, J.-C., Olivier, K., Philippon, A. A., Vourlidas, A., & Yurchyshyn, V. 2012, *A&A* 541, A108.

Wiik, J. E., Dere, K., & Schmieder, B. 1993, *A&A* 273, 267.

Wiik, J. E., Dammasch, I. E., Schmieder, B., & Wilhelm, K. 1999, *Solar Phys.* 187, 405.